BRL

REPORT NO. 1150
SEPTEMBER 1961

THE MAGNUS FORCE ON A ROTATING CYLINDER IN TRANSONIC CROSS FLOWS

A. S. Platou

Department of the Army Project No. 503-03-009
Ordnance Management Structure Code No. 5210.11.140
BALLISTIC RESEARCH LABORATORIES

ABERDEEN PROVING GROUND, MARYLAND

BALLISTIC RESEARCH LABORATORIES

REPORT NO. 1150

SEPTEMBER 1961

THE MAGNUS FORCE ON A ROTATING CYLINDER IN TRANSONIC CROSS FLOWS

A. S. Platou

Exterior Ballistics Laboratory

Department of the Army Project No. 503-03-009
Ordnance Management Structure Code No. 5210.11.140

ABERDEEN PROVING GROUND, MARYLAND

BALLISTIC RESEARCH LABORATORIES

REPORT NO. 1150

ASPlatou/gek
Aberdeen Proving Ground, Md.
September 1961

ABSTRACT

This report presents Magnus and drag data on a rotating cylinder mounted perpendicular to various transonic and supersonic flow fields. Data with both laminar and turbulent boundary layers are presented.

The Magnus force data from the cylinder are compared with Magnus force data from various bodies of revolution at high angles of attack. There is good agreement as long as the body of revolution cross Mach number is transonic. The Magnus force is very much dependent on the cross Mach number at the transonic cross flows. At transonic cross Mach numbers it is possible to predict the Magnus force on a body of revolution by using the presented cylinder data.

TABLE OF CONTENTS

DEFINITION OF SYMBOLS

d	cylinder diameter
b	cylinder span
A	body profile area or cylinder frontal area = d x b
α	angle of attack
ω	cylinder spin rate radians/second
ρ	free stream air density
U	free stream velocity
U_c	cross velocity - the velocity perpendicular to the main axis of a body of revolution $U_c = U \sin \alpha$
M	free stream Mach number
M_c	crossflow Mach number $M_c = M \sin \alpha$
D	drag force
F	Magnus force
k_F	Magnus force coefficient = $\dfrac{F}{\rho U_c^2 A \frac{\omega d}{U_c}}$
C_D	$\dfrac{D}{\frac{1}{2}\rho U^2 A}$ = drag force coefficient

INTRODUCTION

While carrying out Magnus tests on various bodies of revolution, we became aware that the Magnus force is increasingly dependent on the cross Mach number, as the cross Mach number approaches sonic speeds. This can be seen in Figure 1, where the Magnus force coefficient (based on cross flow properties) obtained from wind tunnel tests on various bodies are plotted versus the cross Mach number. Above $M_c = .6$ the force decreases linearly (within reasonable limits) as the cross Mach number increases. This decrease is thought to be brought about by the appearance of sonic cross flow on the body slightly above $M_c = .6$. Once sonic flow appears the forbidden signal rule restricts the flow region influenced by spin. The region of sonic or supersonic flow grows as the cross Mach number increases and the influence of spin becomes less and less.

Our concepts of the generation of the Magnus force at high angles of attack are the same as those expressed in reference 1. Circulation, created by spin, similar to that predicted by the potential theory for a rotating cylinder, cannot occur when the cross flow contains sonic or supersonic flow. Instead, the circulation must be confined to the subsonic portion of boundary layer and the body wake. Also, due to the small size of the boundary layer, it is reasonable to assume that any circulation is confined to the wake and the aft portions of the boundary layer where separation occurs. These regions are on the lee side of the body at an angle of attack and therefore are not readily exposed to the tangential body flow. This may be the reason for the strong dependence of the Magnus force on the cross flow. Since the Magnus force on a body at high angle of attack is dependent mainly on the cross flow it is then quite possible that the Magnus force will correlate well with the Magnus force developed on a cylinder mounted perpendicular to the flow.

In Figure 1 it will be seen that all of the 3 cal. body data above $M_c = .6$ are low compared to the remaining data. In reference 1 it is suggested, using a theory similar to Allen's normal force theory, that the Magnus force on a short body is small due to the short time available for the Magnus force to develop. If this is correct, then it should be better to compare the Magnus force on the aft portion of bodies by subtracting the Magnus force existing on the forward portion of the body. This has been tried with the existing data; however, the resulting accuracy is very bad, and very poor correlation results.

From the above we believed that much could be gained by investigating the Magnus force developed on a rotating cylinder subjected only to a high speed cross flow. The data could be compared to that obtained on bodies of revolution, Figure 1, and also the data should be valuable as data on a basic aerodynamic shape. Also, shadowgraph pictures of the flow region around the cylinder might prove or disprove some of the above statements.

EXPERIMENTAL PROCEDURE

A. Model and Instrumentation

The cylindrical model used for these tests is mounted perpendicular to the tunnel air stream, by supporting the cylinder on the tunnel door mount. The balance for measuring the Magnus and drag forces, the air motor and its bearing are all mounted on the outside of the door, thereby keeping the frontal area of the model to a minimum. Minimum frontal area is necessary to permit operating the tunnel at low supersonic Mach numbers. End plates are used to simulate two-dimensional flow. One end plate is mounted 1-1/2 inches from the tunnel door and is attached to it with the cylinder passing through the end plate. This end plate prevents the tunnel wall boundary layer from affecting the cylinder forces. The second end plate is supported from the tunnel angle of attack system, and serves to create a two-dimensional effect on the end of the cylinder. Neither end plate spins, and the aerodynamic forces created on each are not transmitted to the balance system. A photograph of the cylinder mounted in the test section is shown in Figure 2. The wire braces are for steadying and adjusting the position of the second end plate. The cylinder is 1/2-inch in diameter, the end plates are 8-1/2 inches apart and have radii of 2 inches.

A larger diameter cylinder would have been desirable; however, tunnel blocking* problems at low Mach number forced the use of the small cylinder. A larger cylinder would have created larger Magnus forces and would have permitted larger values of $\omega d/U_c$. The values of $\omega d/U_c$ for the bodies of revolution represented in Figure 1 are up to 1.5 ($M_c > 1$) while the maximum $\omega d/U_c$ ratio for the cylinder data is only .22 . Spin rates up to 250,000 rpm would be necessary with the

*A blocked tunnel is one in which the model is too large for the tunnel and the flow over the model is not the same as would occur in free flight.

1/2-inch diameter cylinder in order to match the spin ratios. These spin rates are impracticable at present and a maximum spin rate of 40,000 rpm was used. However, the obtained cylinder data indicate that the Magnus force is linear with spin and that it is reasonably safe to compare the data independent of the spin ratio.

The air motor and balance systems are shown in Figure 3. The air motor incorporates many of the features used in the previous Magnus tests and is described in Reference 1. The principal difference in this motor is that it is not inclosed within the model, but is attached to one end of the model and is located outside the tunnel. This permits holding the bearing outer races still and spinning the inner races, consequently increasing the bearing life. Also, the balance is external to the air motor and is composed of two cantilevered beams, one measuring the Magnus force and the other the drag force. The balance actually measures a moment due to the Magnus force and a moment due to the drag force; however, by assuming both forces act at the center of the cylinder, the drag and Magnus forces can be obtained.

B. Approaching Two-Dimensional Cylinder Flow

In order to approach two-dimensional flow over the cylinder, end plates have been placed at both ends of the cylinder. 4-inch diameter end plates were found to be sufficient to contain the bow shock at all of the Mach numbers used. However, difficulty arose at the lower Mach numbers due to choking between the door-mounted end plate and the door. Moving the end plate further from the door alleviated this condition to some extent; however, choking still occurred at M = 1.5 and M = 1.4 even with the end plate moved 1-1/2 inches from the wall. However, the Magnus data at M = 1.7 with and without the end plate choking showed very little change, thereby indicating that choking did not have much influence on the Magnus force. Figure 4 shows the effect of choking.

C. Shadowgraph Techniques

Since regular Schlieren and shadowgraph pictures could not be taken, two shadowgraph systems for viewing the flow over the cylinder were devised. The first system involves replacing the door-mounted end plate with an end plate which holds a specially cut (washer shaped) piece of film. The end plate is loaded with film, the test section door is closed and the tunnel started. Once flow is established parallel rays of light, of short duration, are passed through the cylinder flow field onto the film. Necessarily the other end plate is removed and the above sequences are accomplished in a darkened tunnel room.

The shock pattern in front of the cylinder is different during the shadowgraph runs than during the force recording runs, Figure 5. The photographic end plate is 6-inches in diameter while the force measuring end plate is 4-inches in diameter. The photographic end plate could not be made as streamlined, and also the second end plate must be omitted during the shadowgraph runs. Blocking is worse with the photographic end plate and exists at higher Mach numbers than for the force recording end plate. The above accounts for the series of bow shocks seen in the shadowgraphs.

The above technique has certain disadvantages in that the boundary layer surrounding the cylinder cannot be seen. The cylinder is 1/2-inch diameter and the inside hole in the film is 5/8-inch to allow for the cylinder deflection. Also the film is protected from the airstream by lucite also having a 5/8-inch diameter hole. Both of the 5/8-inch holes make it impossible to view the boundary layer around the cylinder.

The washer shaped piece of film is cut from an 8 x 10 piece of film using a "cookie cutter" type stamp. It was necessary to do the cutting in the dark and at times it required more than one hammer blow

to cut the film. On a few of the films the cutter moved between blows leaving rings or marks on the film. In at least one case the film split from the center hole to the outside. Also, the dark, nearly circular spot on each picture is a filled spot in the window.

In most of the photographs an overexposed area extending from the center hole in the film to the outer edge of the film can be seen. This light is apparently reflected from the cylinder onto the film; however, its source is not known. It also occurs on film which is exposed with no flow over the cylinder so that no aerodynamic phenomena is involved.

The second shadowgraph system was devised in order to determine the two-dimensional characteristics of the bow shock, particularly in the vicinity of the end plates. A photographic flashbulb is inclosed in a streamlined metal housing having a No. 80 hole drilled in one side to permit light to escape when the bulb is flashed. The housing is fastened to the tunnel floor so that the No. 80 hole is directly under one of the end plates (see Figure 4). With the tunnel started, and the room darkened, the bulb is flashed, permitting the escaped light to pass through the flow field and expose a sheet of film fastened to the tunnel ceiling.

Figure 4 shows three of this type of shadowgraphs. In most of these pictures the nonuniformity of the light source creates negatives of poor quality which are impossible to use for multiple reproduction. Therefore the flow configurations which are important for this report are either described in the text or sketched as shown in Figure 5.

D. Test Procedure

From the blocking area curve established for the Aberdeen tunnels (ref. 2) it had been expected that the 1/2-inch diamter cylinder could be tested at Mach numbers as low as 1.2 . However, at the start

of testing it was found that M = 1.4 was the lowest supersonic Mach number possible without blocking the tunnel. Since this is at the extreme end of the data in figure 1 it was decided to obtain data at subsonic Mach numbers (M = .6 and M = .8) as well. It was hoped that interpolation in the transonic region would then be possible.

At each Mach number the Magnus and drag data were obtained at four pressure levels or a Reynolds number range from 60,000 to 250,000. The data were automatically recorded on Moseley x-y plotters versus the spin rate (Figure 6) during the coating period of the model-motor combination. Recording of data during the air on (accelerating) period was not possible due to the air turbine forces exerted on the system and the possible air leakage through the door-mounted end plate. To prevent leakage of air from or to the room through the end plate during the data recording a flat disk was placed over the end of the motor during the data gathering period. Data were first obtained on the smooth cylinder at all of the Mach numbers and then data were obtained on the roughened cylinder by gluing No. 40 emery dust to the surface.

The Magnus data obtained on the Moseleys is very erratic (Figure 6). This is due to small extraneous forces exerted on the highly sensitive strain beam by the turbulence in the tunnel flow. The turbulence level in the tunnel supply header is below 1/2% and is not usually noticeable during a test. In this case, due to the small Magnus force involved, the turbulence reduces the accuracy of the Magnus data considerably. Examination of the data indicates that the data are accurate to within $\pm 50\%$ for the supersonic data and within $\pm 10\%$ for the subsonic data. The subsonic data are more accurate due to the increased magnitude.

RESULTS AND DISCUSSION

The Magnus force generated on the smooth surfaced cylinder is linear with spin within the accuracy of the data and is not influenced by Reynolds number in the range covered (the two data points in Figure 7 at each Mach number represent the data spread over the Re range). The force decreases rapidly as the Mach number increases (Figure 7), and reaches a constant minimum value as soon as or shortly after the cross Mach number becomes supersonic. The shadowgraphs (Figures 8a and 8b) show that spin has no noticeable influence on the wake as long as the flow is supersonic, but has a slight influence on the flow regions surrounding the cylinder at subsonic speeds. At higher peripheral speeds, which are not attainable with this model, the shadowgraphs should show a much more noticeable effect at the subsonic speeds. The wake just downstream of the cylinder, both with and without spin, has very sharply defined limits suggesting that the cylinder boundary layer is laminar. Further evidence of a laminar boundary layer is seen in the drag data where the drag agrees well with the drag data from reference 3 (Figure 9). It should also be noted that throughout the tests the drag did not vary with spin.

In Figure 10 the Magnus data from the cylinder are compared with the data (Figure 1) obtained from various bodies of revolution at various cross flow Mach numbers. It is seen that the data are of the same order of magnitude from $M = .8$ to $M = 1.4$. This is the region in which we expected agreement if the cross flow theory stated in the introduction is true. It is also expected that if data at higher cross flow Mach numbers had been available it would agree with the higher Mach number cylinder data.

Results on the rough surfaced cylinder are quite surprising and are not fully understood. The Magnus data are similar to those for

the smooth surfaced cylinder except that the Magnus force is negative* at the supersonic velocities (Figure 7). The Magnus data are linear with spin and do not vary over the Reynolds number range covered. The negative Magnus force absolute values are approximately the same as the smooth surfaced cylinder values and at subsonic speeds both surface cases have positive Magnus forces of equal value. The shadowgraphs again show that spin does not influence the flow pattern (Figures 11a and 11b), except at subsonic speeds. The wake is not as clearly defined as with the smooth surfaced cylinder and the wake is wider at its narrowest point. Further evidence of a turbulent boundary layer is that the turbulent drag at subsonic speeds is less than the laminar drag (Figure 9).

Reference 4 presents Magnus data on a 3-inch diameter smooth surfaced cylinder obtained in the Naval Ordnance Laboratory Tunnel No. 1. These data cover the Mach number range from 1.75 to 3.24 and a Reynolds number range from $.55 \times 10^6$ to 1.06×10^6. These data are compared with the BRL data in Figures 7 and 9 and excellent agreement is obtained for both Magnus force and drag force. It shows that the Magnus force coefficient is constant, in the supersonic region, over a larger Reynolds number range than shown separately by the two sets of data. The NOL data at M = 1.75 have not been shown for it has recently been determined by the Navy that the flow over the model at M = 1.75 is questionable.

*A negative Magnus force acts in the opposite direction from that predicted by the potential theory for the lift (Magnus force) on a rotating cylinder. In Figure 8 the positive Magnus force direction is down.

CONCLUSIONS

1. Correlation does exist between the Magnus force on a body of revolution in transonic or supersonic cross flows and the Magnus force on a rotating cylinder whose centerline is perpendicular to the airstream.

2. The body axial flow, M cos α, has little or no influence on the Magnus force.

3. The Magnus force on the smooth surfaced cylinder (laminar boundary layer) is positive at all Mach numbers tested. The Magnus force on the rough surfaced cylinder (turbulent boundary layer) is positive at subsonic velocities, bu negative at supersonic velocities.

4. The drag is not influenced by spin within the accuracy of measurement.

5. It is possible to predict the Magnus force on any body of revolution in transonic cross flows by using the presented rotating cylinder data.

Anders S Platou

ANDERS S. PLATOU

REFERENCES

1. Platou, A. S. and Sternberg, J. The Magnus Characteristics of a 30-mm Aircraft Bullet. BRL Report No. 994, 1956.

2. Bluestone, E. Flexible Nozzle Tunnel No. 3 - Model Design Criteria and Tunnel Operating Conditions. BRL Memorandum Report No. 711, 1953.

3. Gowen, Forrest E. and Perkins, Edward W. Drag of Circular Cylinders for a Wide Range of Reynolds Numbers and Mach Numbers. NACA TN No. 2960.

4. Hall, R. T. The Lift and Drag on a Rotating Cylinder in Supersonic Crossflow. NAVORD Report No. 6039, 1960.

MAGNUS FORCE VERSUS CROSS FLOW MACH NO.

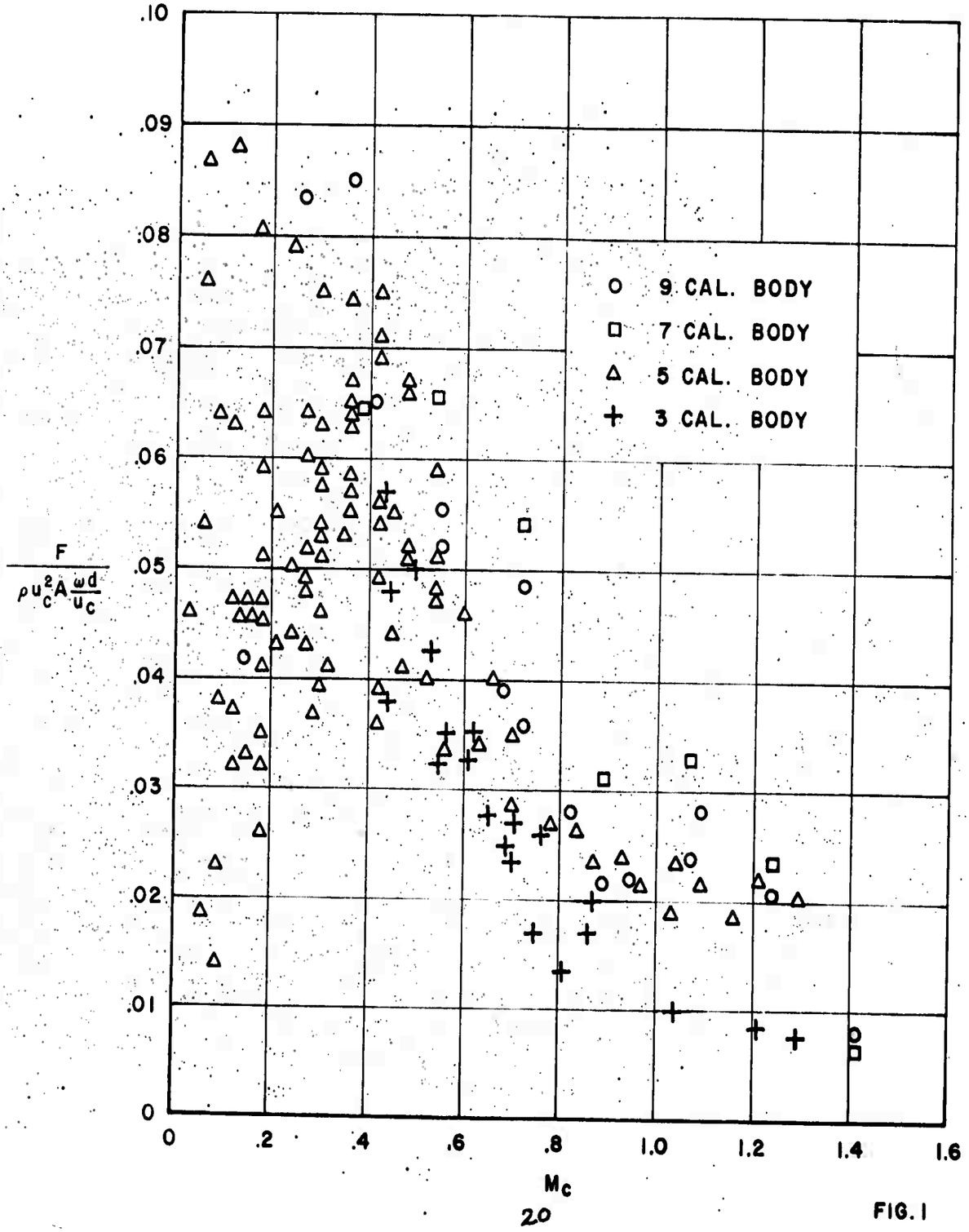

FIG. 1

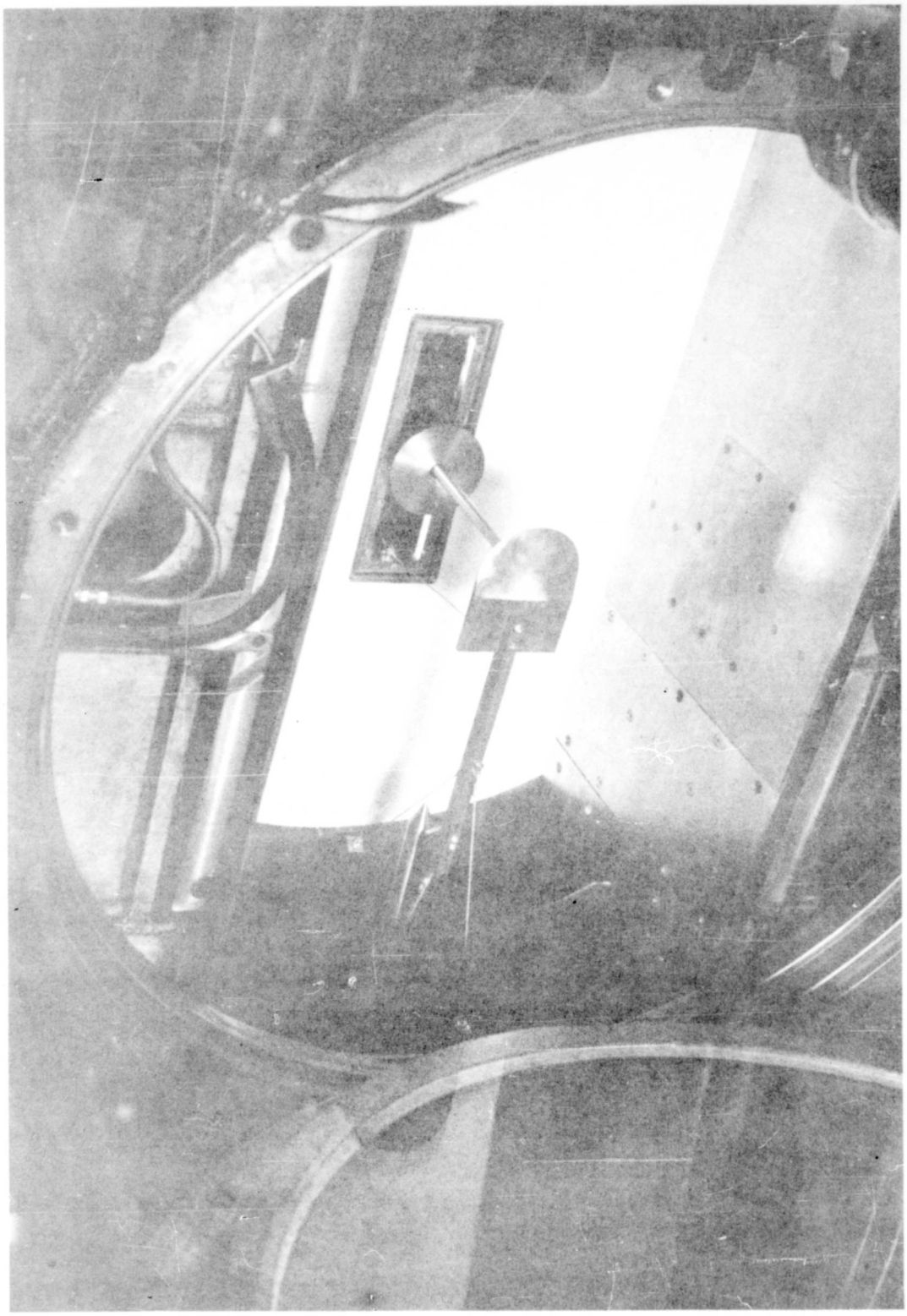

FIG. 2 The Cylinder Mounted in the Test Section

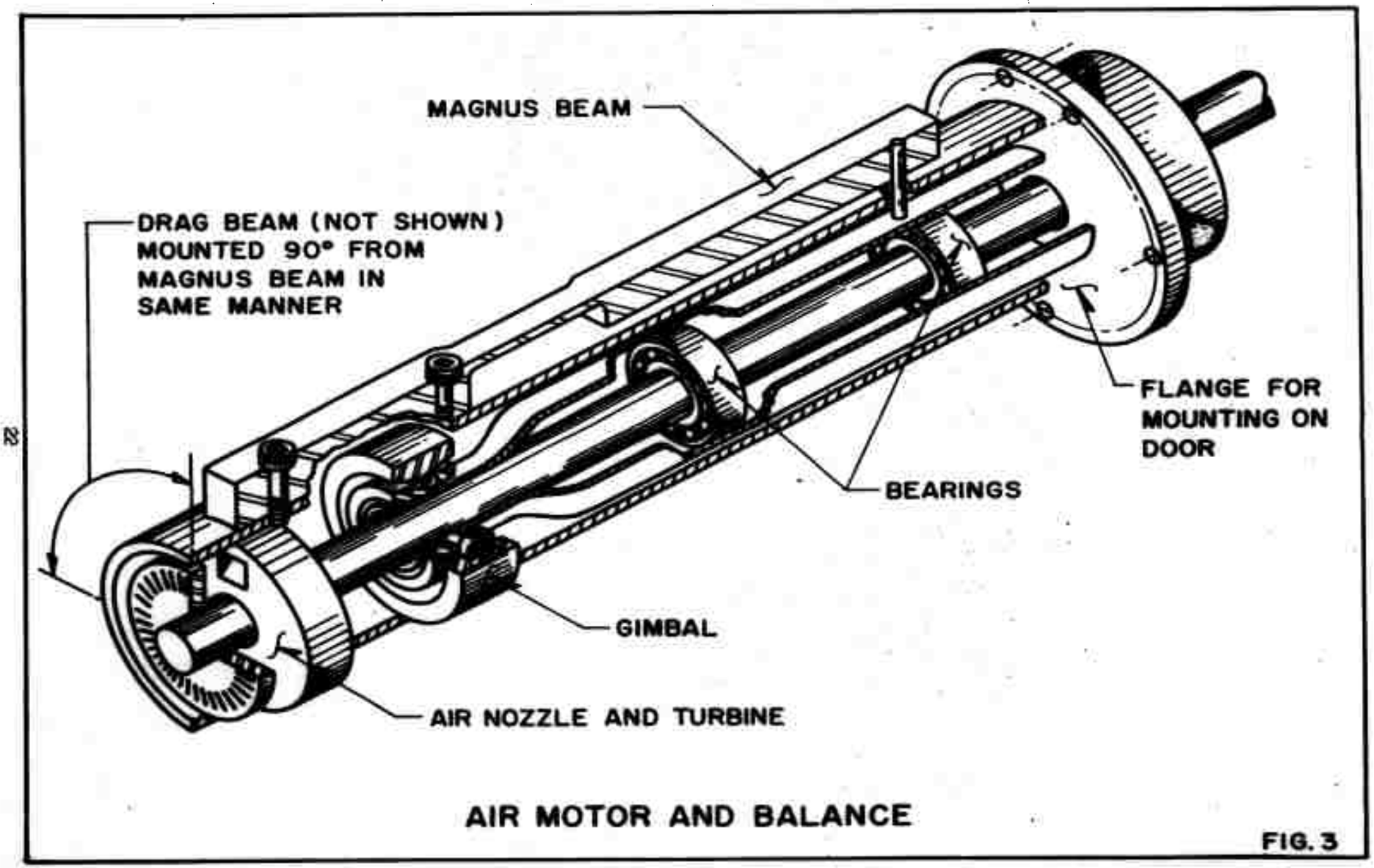

AIR MOTOR AND BALANCE

FIG. 3

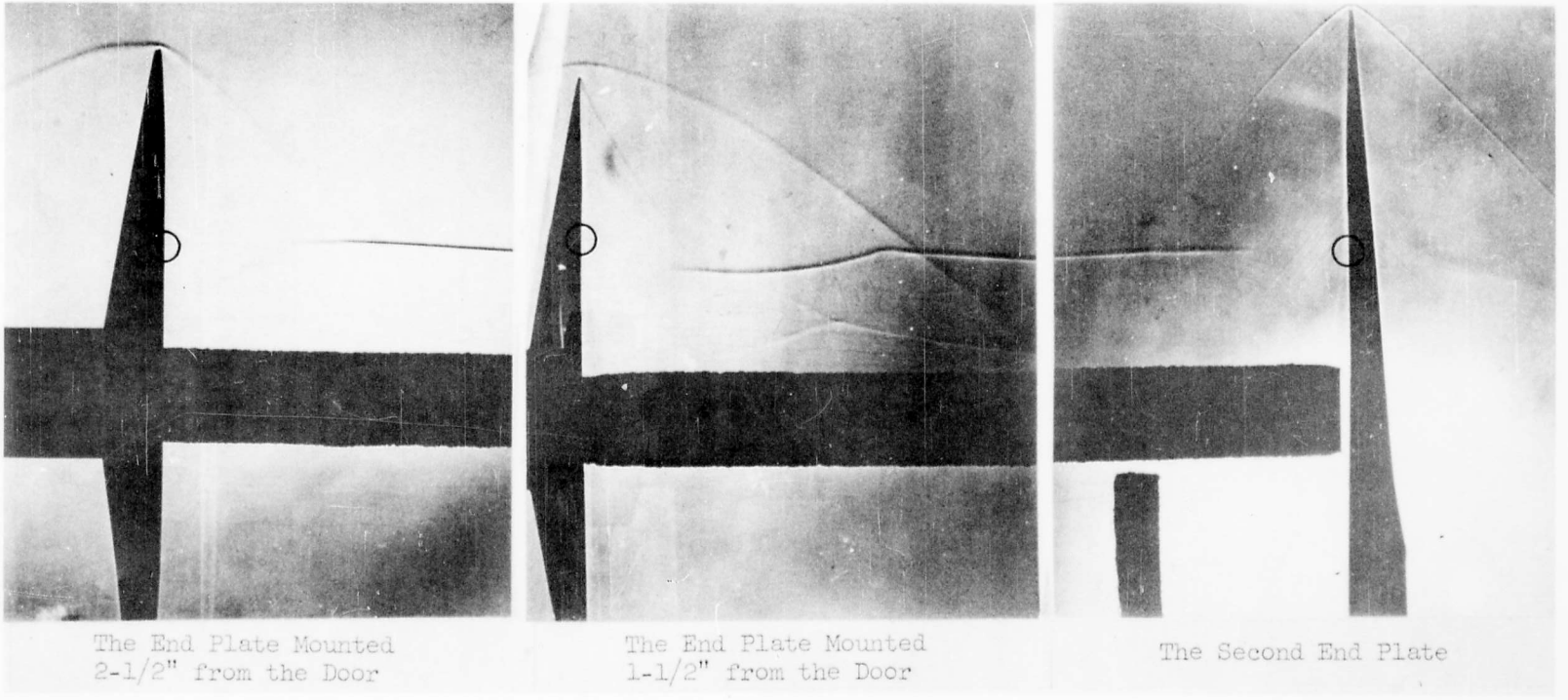

The End Plate Mounted 2-1/2" from the Door

The End Plate Mounted 1-1/2" from the Door

The Second End Plate

FIG. 4 The Flow at the Cylinder Ends
○ marks approx. location of No. 80 hole

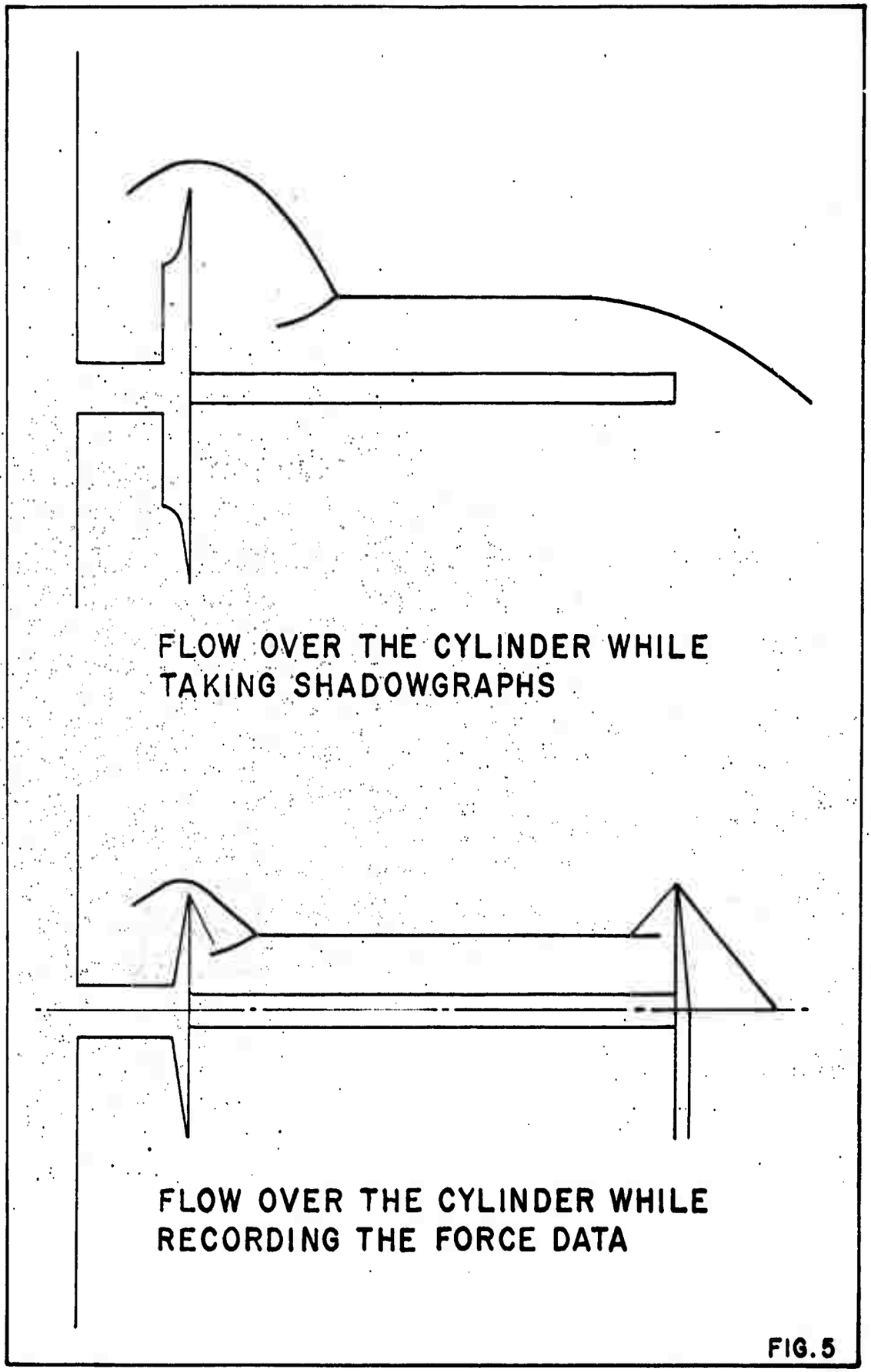
FLOW OVER THE CYLINDER WHILE
TAKING SHADOWGRAPHS
FLOW OVER THE CYLINDER WHILE
RECORDING THE FORCE DATA

FIG. 5

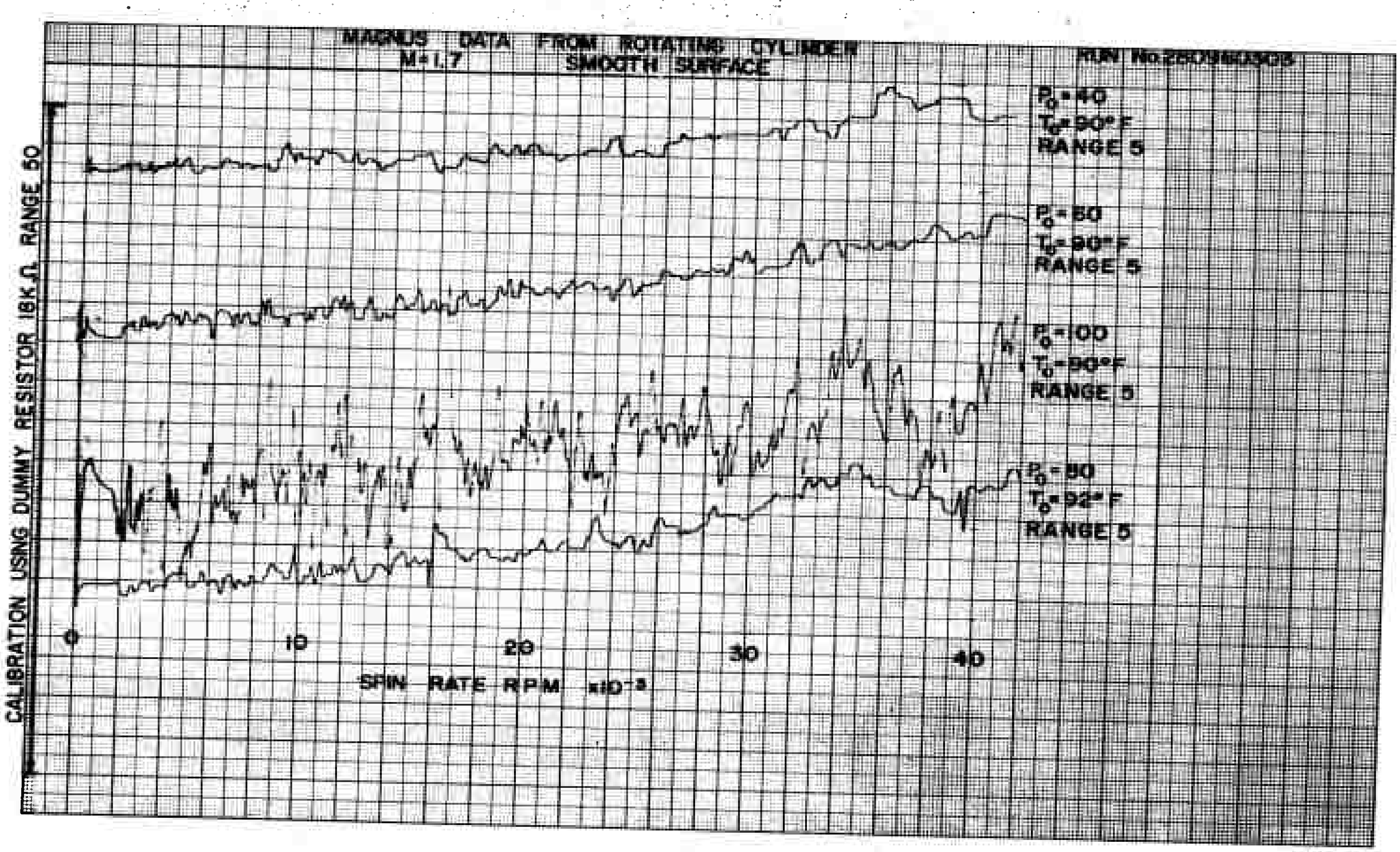
MAGNUS DATA FROM ROTATING CYLINDER
M = 1.7
SMOOTH SURFACE
RUN No.
P_o = 40
T_o = 90° F
RANGE 5
P_o = 60
T_o = 90° F
RANGE 5
P_o = 100
T_o = 90° F
RANGE 5
P_o = 80
T_o = 92° F
RANGE 5
CALIBRATION USING DUMMY RESISTOR 18K Ω RANGE 50
0
10
20
30
40
SPIN RATE RPM x10⁻³

FIG. 6

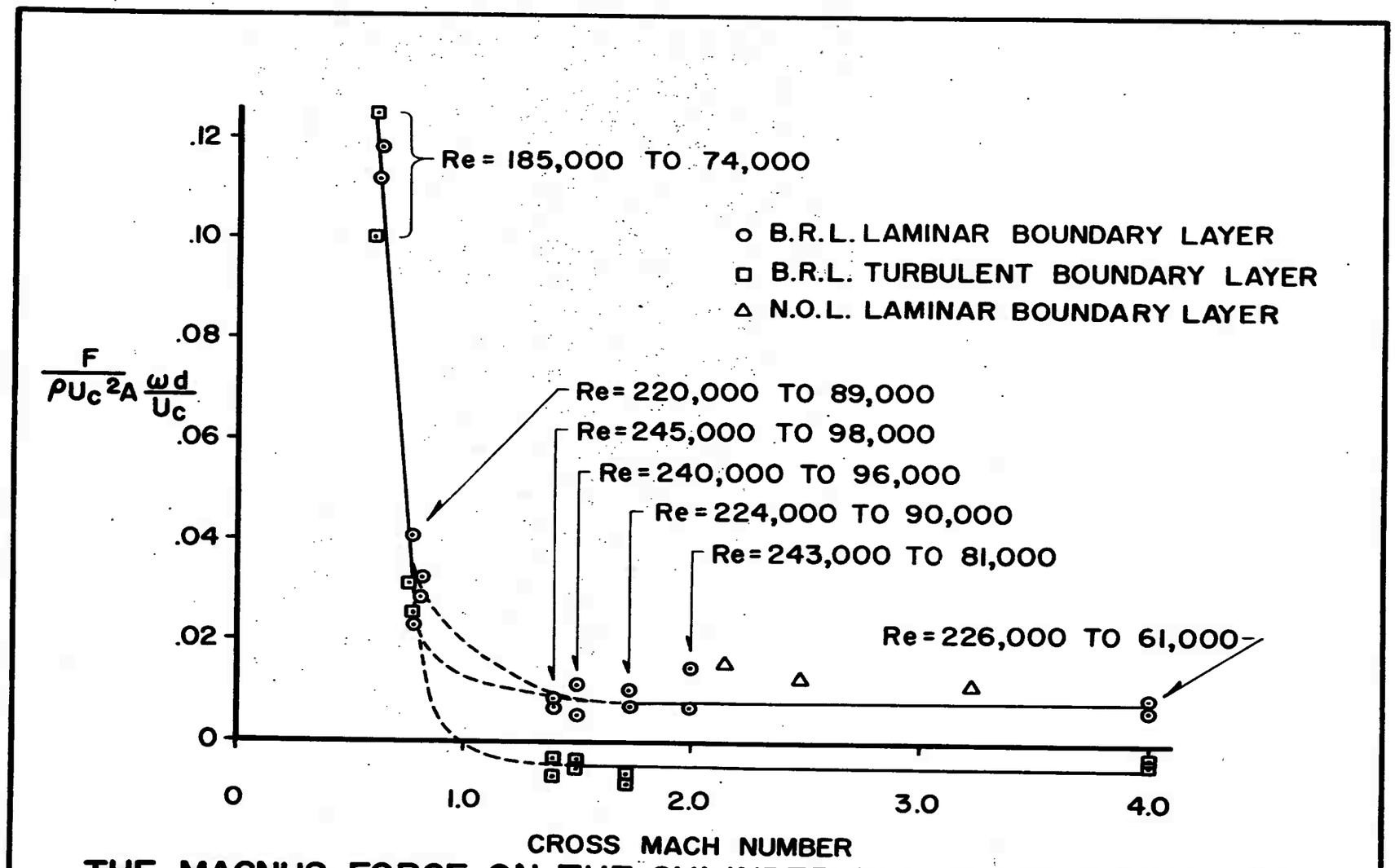

THE MAGNUS FORCE ON THE CYLINDER VERSUS THE MACH NO.

FIG. 7

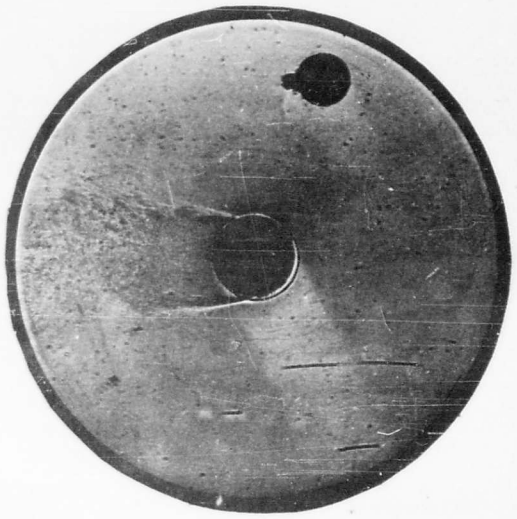

M = .6
$\frac{\omega d}{U} = 0$

M = .6
$\frac{\omega d}{U} = .217$

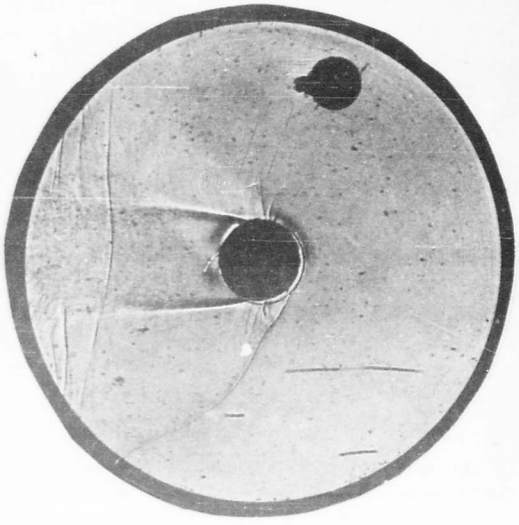

M = .8
$\frac{\omega d}{U} = 0$

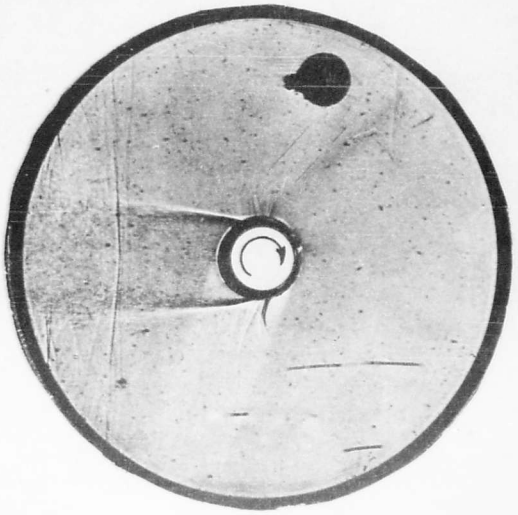

M = .8
$\frac{\omega d}{U} = .132$

THE FLOW OVER THE SMOOTH SURFACED CYLINDER

FIG. 8a

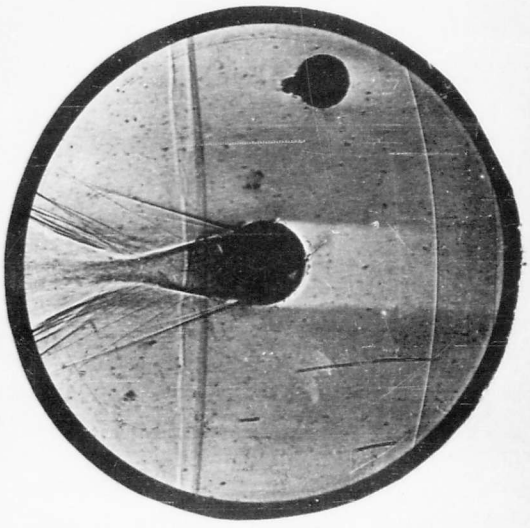

M = 1.4
$\frac{\omega d}{U} = 0$

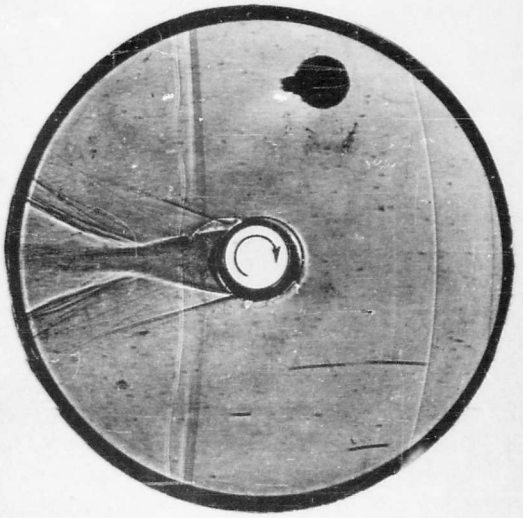

M = 1.4
$\frac{\omega d}{U} = .128$

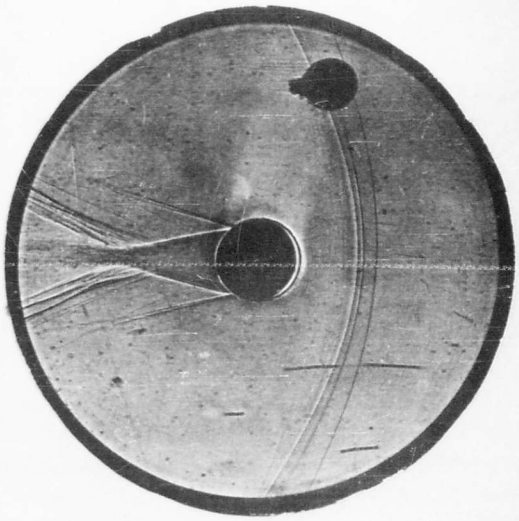

M = 1.7
$\frac{\omega d}{U} = 0$

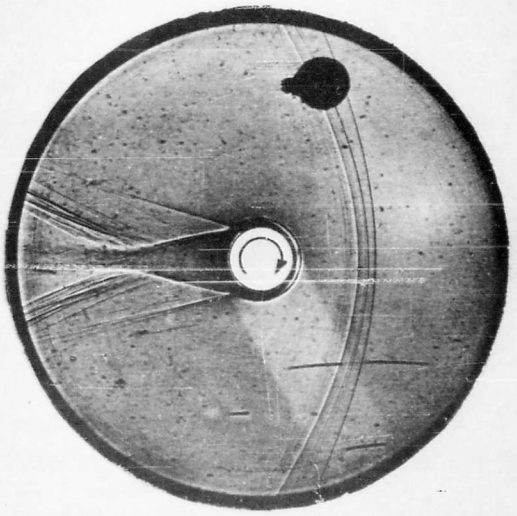

M = 1.7
$\frac{\omega d}{U} = .122$

THE FLOW OVER THE SMOOTH SURFACED CYLINDER

FIG. 8b

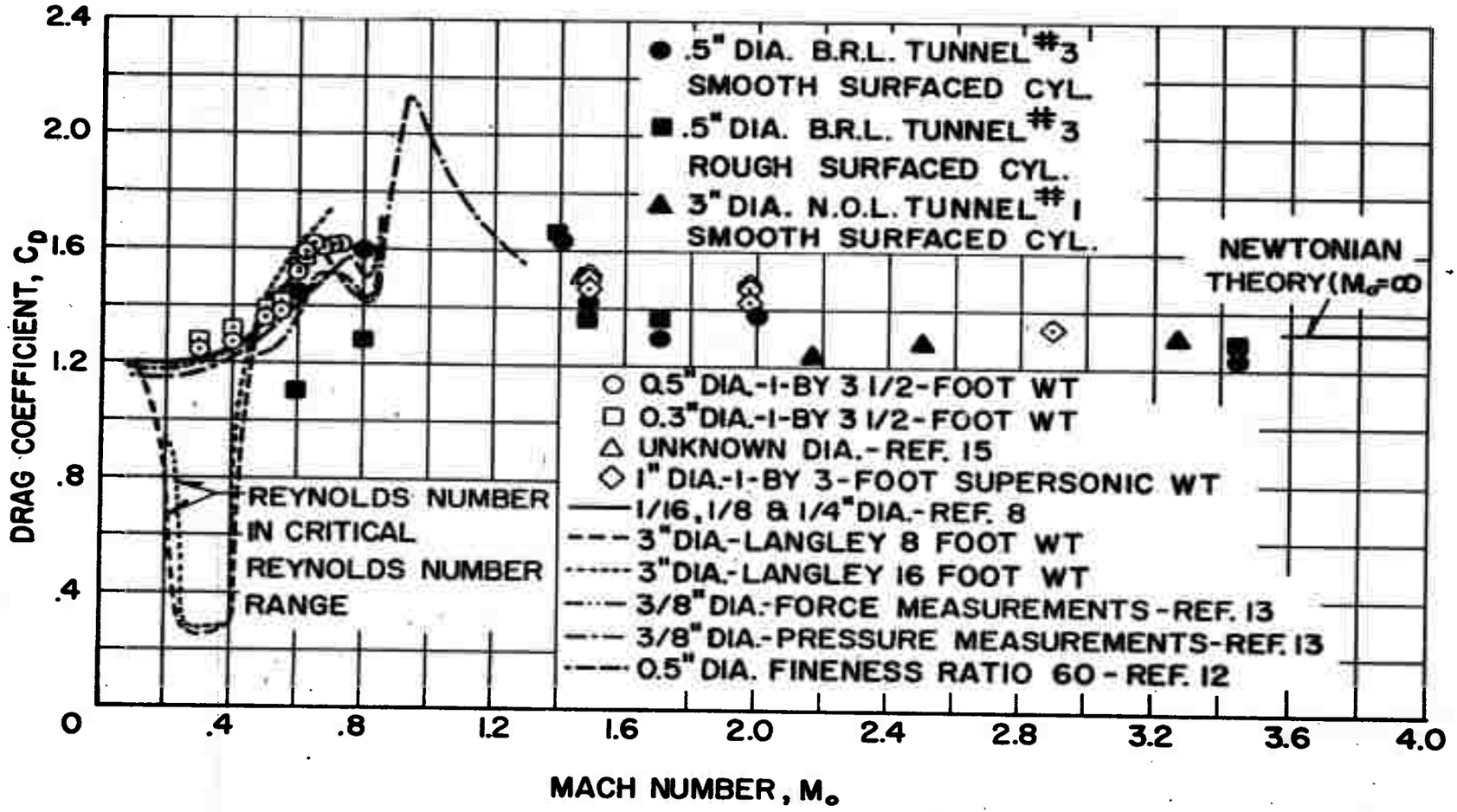

THE EFFECT OF MACH NUMBER ON CIRCULAR-CYLINDER DRAG COEFFICIENTS

FIG. 9

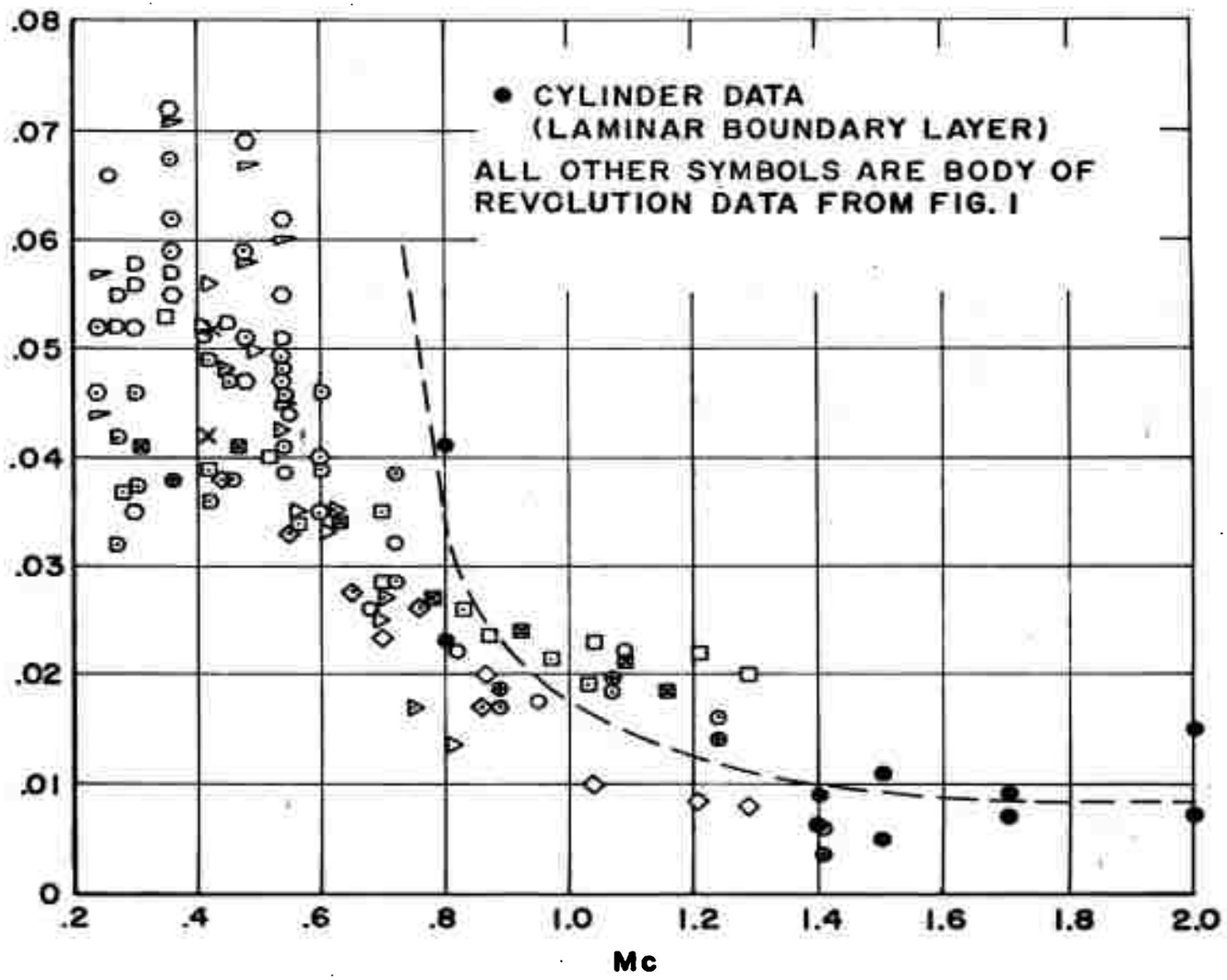

COMPARISON OF THE CYLINDER DATA WITH THE BODY OF REVOLUTION DATA

FIG. 10

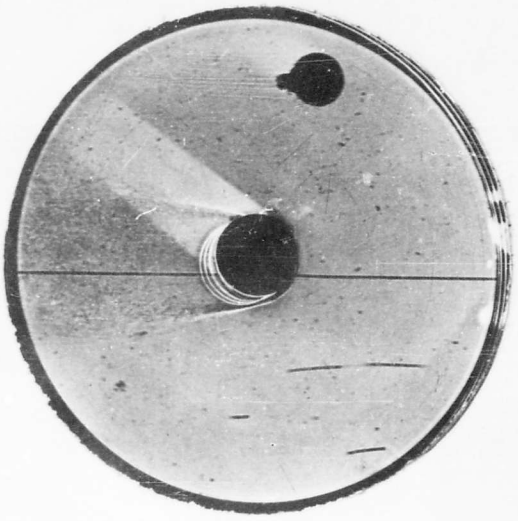

M = .6
$\frac{\omega d}{U} = 0$

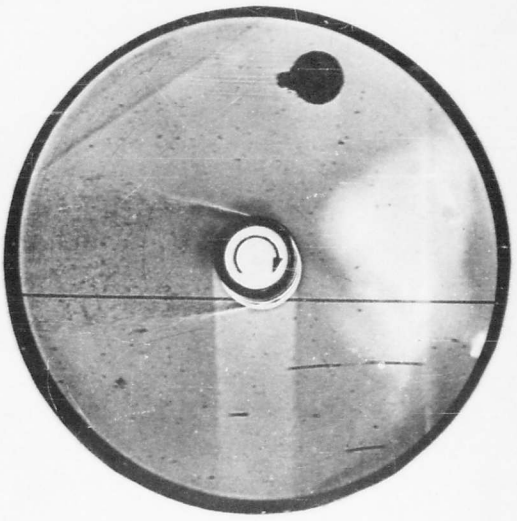

M = .6
$\frac{\omega d}{U} = .217$

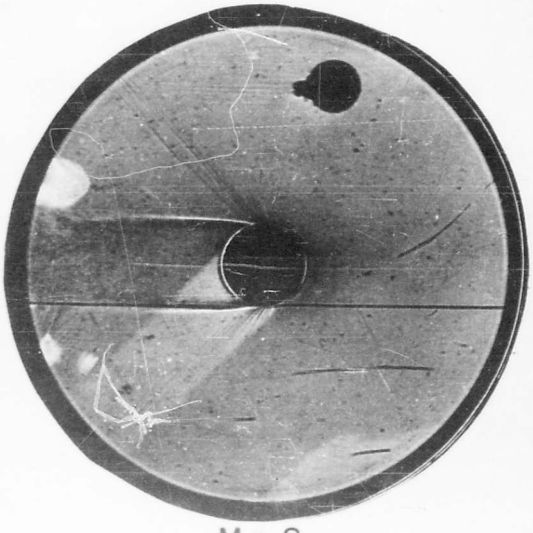

M = .8
$\frac{\omega d}{U} = 0$

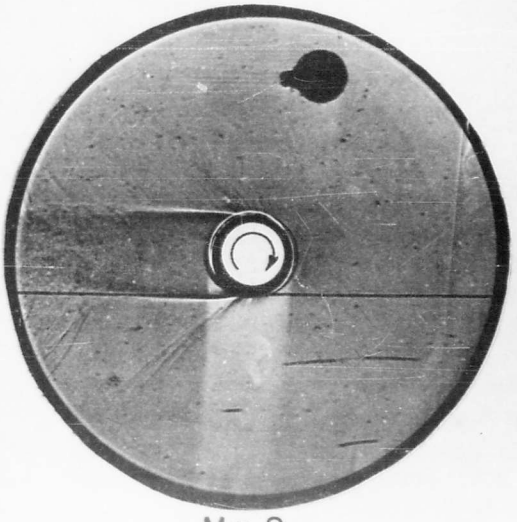

M = .8
$\frac{\omega d}{U} = .132$

THE FLOW OVER THE ROUGH SURFACED CYLINDER

FIG. 11a

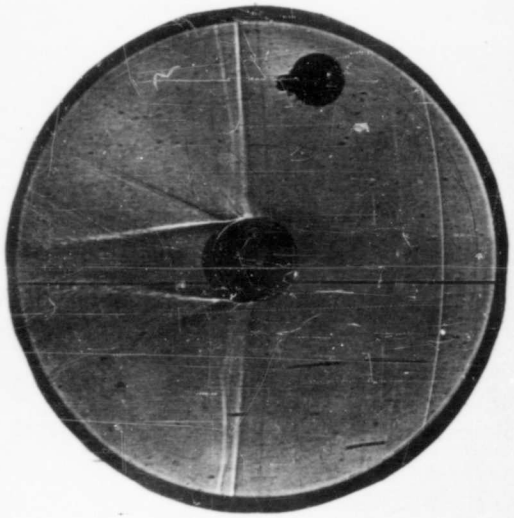

M = 1.4
$\frac{\omega d}{U} = 0$

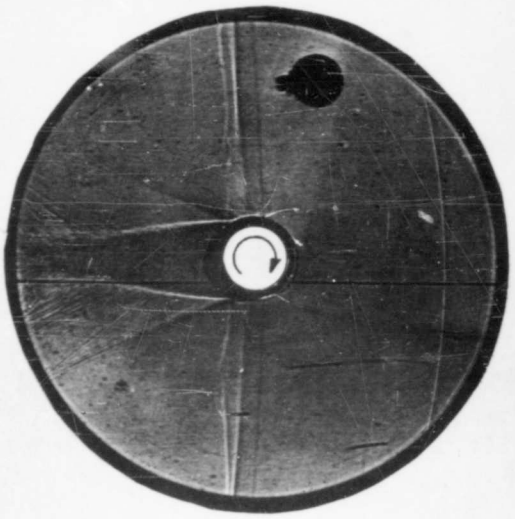

M = 1.4
$\frac{\omega d}{U} = .128$

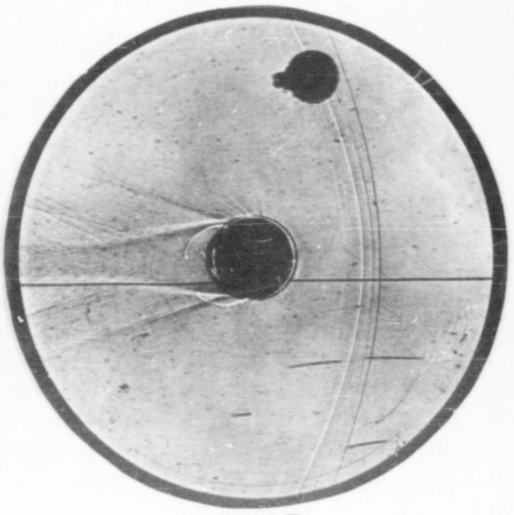

M = 1.7
$\frac{\omega d}{U} = 0$

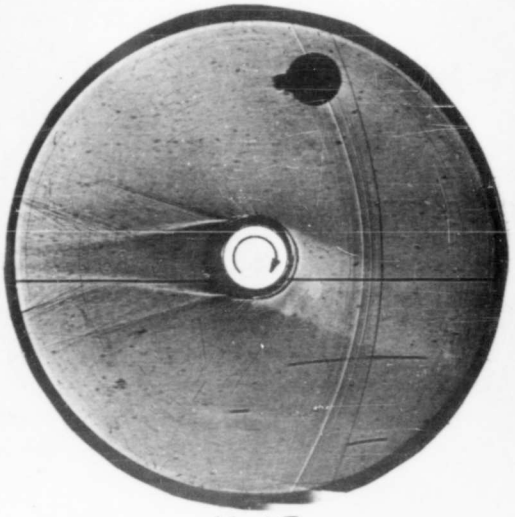

M = 1.7
$\frac{\omega d}{U} = .122$

THE FLOW OVER THE ROUGH SURFACED CYLINDER

FIG. 11b

DISTRIBUTION LIST

No. of Copies	Organization
1	Chief of Ordnance ATTN: ORDTB - Bal Sec Department of the Army Washington 25, D.C.
10	Commanding Officer Army Research Office (Durham) Box CM, Duke Station Durham, North Carolina
1	Chief of Research & Development ATTN: Army Research Office Department of the Army Washington 25, D.C.
3	Chief, Bureau of Naval Weapons ATTN: DIS-33 Department of the Navy Washington 25, D.C.
1	Commander U.S. Naval Ordnance Test Station ATTN: Dr. H.R. Kelley China Lake, California
2	Commander Naval Ordnance Laboratory ATTN: Dr. Kurzweg Dr. E. Krahn White Oak Silver Spring 19, Maryland
1	Naval Supersonic Laboratory Massachusetts Institute of Technology ATTN: Mr. Frank H. Durgin 560 Memorial Drive Cambridge 39, Massachusetts
1	Commander Air Proving Ground Center ATTN: Mr. Foster Burgess Eglin Air Force Base, Florida
1	Commander Ballistic Systems Division Air Force Unit Post Office Los Angeles 45, California
1	Commander Air Force Special Weapons Center ATTN: SWK SWUND, Major D. Schumucker Kirtland Air Force Base, New Mexico
2	Director National Aeronautics and Space Administration ATTN: Mr. H.J. Allen Dr. A. Eggers Ames Research Center Moffett Field, California
3	Director National Aeronautics and Space Administration ATTN: Mr. J. Bird Mr. C.E. Brown Dr. A. Buseman Langley Research Center Langley Field, Virginia
1	Director National Aeronautics and Space Administration ATTN: Dr. Evaard Lewis Research Center Cleveland Airport Cleveland, Ohio
1	Director National Bureau of Standards ATTN: Mr. G.B. Schubauer 232 Dynamometer Building Washington 25, D.C.

DISTRIBUTION LIST

No. of Copies	Organization
1	Aerophysics Development Corporation P.O. Box 657 Pacific Palisades, California
1	ARO, Inc. ATTN: Mr. R. Smelt P.O. Box 162 Tullahoma, Tennessee
1	AVCO Everett Research Laboratories ATTN: Mr. Stankevies 2385 Revere Beach Parkway Everett 49, Massachusetts
1	The Budd Company ATTN: Ordnance Research Department 2450 Hunting Park Avenue Philadelphia 15, Pennsylvania
1	Chamberlain Corporation ATTN: Mr. Irving Herman Waterloo, Iowa
2	Cornell Aeronautical Laboratory, Inc. ATTN: Dr. A. Flaz Dr. Ira G. Ross Buffalo, New York
1	The Eglin Corporation ATTN: Dr. Floyd. L. Cash 2925 Merrill Road P.O. Box 13214 Dallas 20, Texas
1	General Electric Research Laboratories ATTN: Library P.O. Box 1088 Schenectady, New York
1	Grumman Aircraft Engineering Corporation ATTN: Mr. C. Tilgner, Jr. Bethpage, Long Island, New York
1	Hercules Powder Company, Inc. Allegany Ballistics Laboratory Cumberland, Maryland
1	I.T.T. Federal Laboratories Division of International Telephone and Telegraph Corporation ATTN: Technical Library 3700 East Pontiac Fort Wayne, Indiana
1	Jet Propulsion Laboratory ATTN: Dr. F. Goddard 4800 Oak Grove Drive Pasadena, California
1	North American Aviation, Inc. ATTN: Dr. E. C. Van Driest Aeronautical Laboratory Downey, California
1	Ramo-Wooldridge Corporation ATTN: Dr. Louis G. Dunn 409 East Manchester Boulevard Inglewood, California
1	Space Technology Laboratories, Inc. ATTN: Dr. H. Zuckerberg, Special Projects Department P.O. Box 95001 Los Angeles 45, California
1	United Aircraft Corporation ATTN: Mr. M. Schweiger East Hartford, Connecticut
1	Wright Aeronautical Division Curtiss-Wright Corporation ATTN: Technical Library Wood-Ridge, New Jersey

DISTRIBUTION LIST

No. of Copies	Organization
1	Brown University ATTN: Dr. R. Probstein Graduate Division of Applied Mathematics Providence 12, Rhode Island
1	Catholic University of America ATTN: Professor K.F. Herzfeld Professor M. Monk Department of Physics Washington 17, D.C.
1	Case Institute of Technology ATTN: Dr. G. Kuerti Cleveland, Ohio
1	California Institute of Technology Guggenheim Aeronautical Laboratory ATTN: Professor H.W. Liepman Pasadena 4, California
1	University of California at Berkeley ATTN: Professor S.A. Schaaf Berkeley, California
1	University of California at Los Angeles ATTN: Dr. L.M. Boelter Department of Engineering Los Angeles 24, California
2	Cornell University ATTN: Dr. A. Kantrowitz Dr. W.R. Sears Graduate School of Aeronautical Engineering Ithaca, New York
1	Harvard University ATTN: Dr. A. Bryson Department of Applied Physics & Engineering Science Cambridge 38, Massachusetts
1	University of Illinois ATTN: Professor C.H. Fletcher Department of Aeronautical Engineering Urbana, Illinois
1	Institute of the Aeronautical Sciences ATTN: Library 2 East 64th Street New York 21, New York
2	The Johns Hopkins University ATTN: Dr. L. Kosvasznay - Department of Aeronautical Engineering Dr. S. Corrsin - Department of Mechanical Engineering Baltimore 18, Maryland
1	Lehigh University ATTN: Dr. R. Emrich Physics Department Bethlehem, Pennsylvania
2	University of Maryland ATTN: Director, Institute of Fluid Dynamics and Applied Mathematics Dr. S.F. Shen - Department of Aeronautical Engineering College Park, Maryland

DISTRIBUTION LIST

No. of Copies	Organization
1	Massachusetts Institute of Technology ATTN: Professor J.R. Markham Department of Aeronautical Engineering Cambridge 39, Massachusetts
1	University of Michigan ATTN: Dr. Arnold Kuethe Department of Aeronautical Engineering East Engineering Building Ann Arbor, Michigan
2	University of Minnesota ATTN: Department of Aeronautical Engineering - Dr. R. Hermann Department of Mechanical Engineering, Division of Thermodynamics - Dr. E.R.G. Eckert Minneapolis 14, Minnesota
1	Midwest Research Institute ATTN: Mr. M. Goland, Director for Engineering Sciences 4049 Pennsylvania Kansas City 11, Missouri
1	National Science Foundation ATTN: Dr. R. Seeger Washington 25, D.C.
2	New York University ATTN: Dr. R.W. Courant - Institute of Mathematics & Mechanics Dr. J.F. Ludloff - Department of Aeronautics 45 Fourth Street New York 53, New York
1	North Carolina State College ATTN: Professor R.M. Pinkerton Department of Engineering Releigh, North Carolina
1	Ohio State University ATTN: Professor G.L. von Eschen Aeronautical Engineering Department Columbus, Ohio
1	Pennsylvania State College ATTN: Professor M. Lessen Department of Aeronautical Engineering State College, Pennsylvania
1	Polytechnic Institute of Brooklyn ATTN: Dr. A. Ferri Aerodynamic Laboratory 527 Atlantic Avenue Freeport, New York
2	Princeton University ATTN: Professor S. Bogdonoff Professor W. Hayes Forrestal Research Center Princeton, New Jersey
1	Rensselaer Polytechnic Institute ATTN: Dr. R.P. Harrington Aeronautics Department Troy, New York
1	University of Texas Defense Research Laboratory ATTN: Mr. J.B. Oliphint P.O. Box 8029 University Station Austin 12, Texas

DISTRIBUTION LIST

No. of Copies	Organization
1	University of Washington ATTN: Professor R.E. Street Department of Aeronautical Engineering Seattle 5, Washington
1	Professor J.W. Beams University of Virginia Department of Physics Charlottesville, Virginia
1	Dr. R. Bolz Case Institute of Technology Cleveland, Ohio
1	Professor G.F. Carrier Harvard University Division of Engineering and Applied Physics Cambridge 38, Massachusetts
1	Professor F.H. Clauser, Jr. Chairman, Department of Aeronautics The Johns Hopkins University Baltimore 18, Maryland
1	Professor H.W. Emmons Harvard University Cambridge 38, Massachusetts
1	Mr. Gerald Hieser Systems Engineering Department General Electric Company 21 South 12th Street Room 514 Philadelphia, Pennsylvania
1	Professor J.O. Hirschfelder University of Wisconsin Department of Chemistry Madison, Wisconsin
1	Professor C.B. Millikan Director, Guggenheim Aeronautical Laboratory California Institute of Technology Pasadena 4, California
1	Professor William Prager Chairman, Physical Sciences Council Brown University Providence 12, Rhode Island
10	Commander British Army Staff British Defence Staff (W) ATTN: Reports Officer 3100 Massachusetts Avenue, N.W. Washington 8, D.C.
4	Defence Research Member Canadian Joint Staff 2450 Massachusetts Avenue, N.W. Washington 8, D.C.
189	GM/MML - 200/23, dtd 3 Apr 61 Parts A,C and DA

AD _____ Accession No. _____

Ballistic Research Laboratories, ARG

THE MAGNUS FORCE ON A ROTATING CYLINDER IN TRANSONIC CROSS FLOWS

A. S. Platou

BRL Report No. 1150, September 1961

DA Proj No. 503-03-009, OMSC No. 5210.11.140

UNCLASSIFIED Report

UNCLASSIFIED

Projectiles - Exterior Ballistics -Measurements
Projectiles - Aerodynamic Characteristics

This report presents Magnus and drag data on a rotating cylinder mounted perpendicular to various transonic and supersonic flow fields. Data with both laminar and turbulent boundary layers are presented.

The Magnus force data from the cylinder are compared with Magnus force data from various bodies of revolution at high angles of attack. There is good agreement as long as the body of revolution cross Mach number is transonic. The Magnus force is very much dependent on the cross Mach number at the transonic cross flows. At transonic cross Mach numbers it is possible to predict the Magnus force on a body of revolution by using the presented cylinder data.

AD _____ Accession No. _____

Ballistic Research Laboratories, ARG

THE MAGNUS FORCE ON A ROTATING CYLINDER IN TRANSONIC CROSS FLOWS

A. S. Platou

BRL Report No. 1150, September 1961

DA Proj No. 503-03-009, OMSC No. 5210.11.140

UNCLASSIFIED Report

UNCLASSIFIED

Projectiles - Exterior Ballistics -Measurements
Projectiles - Aerodynamic Characteristics

This report presents Magnus and drag data on a rotating cylinder mounted perpendicular to various transonic and supersonic flow fields. Data with both laminar and turbulent boundary layers are presented.

The Magnus force data from the cylinder are compared with Magnus force data from various bodies of revolution at high angles of attack. There is good agreement as long as the body of revolution cross Mach number is transonic. The Magnus force is very much dependent on the cross Mach number at the transonic cross flows. At transonic cross Mach numbers it is possible to predict the Magnus force on a body of revolution by using the presented cylinder data.

AD _____ Accession No. _____

Ballistic Research Laboratories, ARG

THE MAGNUS FORCE ON A ROTATING CYLINDER IN TRANSONIC CROSS FLOWS

A. S. Platou

BRL Report No. 1150, September 1961

DA Proj No. 503-03-009, OMSC No. 5210.11.140

UNCLASSIFIED Report

UNCLASSIFIED

Projectiles - Exterior Ballistics -Measurements
Projectiles - Aerodynamic Characteristics

This report presents Magnus and drag data on a rotating cylinder mounted perpendicular to various transonic and supersonic flow fields. Data with both laminar and turbulent boundary layers are presented.

The Magnus force data from the cylinder are compared with Magnus force data from various bodies of revolution at high angles of attack. There is good agreement as long as the body of revolution cross Mach number is transonic. The Magnus force is very much dependent on the cross Mach number at the transonic cross flows. At transonic cross Mach numbers it is possible to predict the Magnus force on a body of revolution by using the presented cylinder data.

AD Accession No.
Ballistic Research Laboratories, APG
THE MAGNUS FORCE ON A ROTATING CYLINDER IN TRANSONIC CROSS FLOWS
A. S. Platou

BRL Report No. 1150, September 1961

DA Proj No. 503-03-009, OMSC No. 5210.11.140
UNCLASSIFIED Report

UNCLASSIFIED

Projectiles - Exterior Ballistics - Measurements
Projectiles - Aerodynamic Characteristics

This report presents Magnus and drag data on a rotating cylinder mounted perpendicular to various transonic and supersonic flow fields. Data with both laminar and turbulent boundary layers are presented.

The Magnus force data from the cylinder are compared with Magnus force data from various bodies of revolution at high angles of attack. There is good agreement as long as the body of revolution cross Mach number is transonic. The Magnus force is very much dependent on the cross Mach number at the transonic cross flows. At transonic cross Mach numbers it is possible to predict the Magnus force on a body of revolution by using the presented cylinder data.

AD Accession No.
Ballistic Research Laboratories, APG
THE MAGNUS FORCE ON A ROTATING CYLINDER IN TRANSONIC CROSS FLOWS
A. S. Platou

BRL Report No. 1150, September 1961

DA Proj No. 503-03-009, OMSC No. 5210.11.140
UNCLASSIFIED Report

UNCLASSIFIED

Projectiles - Exterior Ballistics-Measurements
Projectiles - Aerodynamic Characteristics

This report presents Magnus and drag data on a rotating cylinder mounted perpendicular to various transonic and supersonic flow fields. Data with both laminar and turbulent boundary layers are presented.

The Magnus force data from the cylinder are compared with Magnus force data from various bodies of revolution at high angles of attack. There is good agreement as long as the body of revolution cross Mach number is transonic. The Magnus force is very much dependent on the cross Mach number at the transonic cross flows. At transonic cross Mach numbers it is possible to predict the Magnus force on a body of revolution by using the presented cylinder data.

AD Accession No.
Ballistic Research Laboratories, APG
THE MAGNUS FORCE ON A ROTATING CYLINDER IN TRANSONIC CROSS FLOWS
A. S. Platou

BRL Report No. 1150, September 1961

DA Proj No. 503-03-009, OMSC No. 5210.11.140
UNCLASSIFIED Report

UNCLASSIFIED

Projectiles - Exterior Ballistics - Measurements
Projectiles - Aerodynamic Characteristics

This report presents Magnus and drag data on a rotating cylinder mounted perpendicular to various transonic and supersonic flow fields. Data with both laminar and turbulent boundary layers are presented.

The Magnus force data from the cylinder are compared with Magnus force data from various bodies of revolution at high angles of attack. There is good agreement as long as the body of revolution cross Mach number is transonic. The Magnus force is very much dependent on the cross Mach number at the transonic cross flows. At transonic cross Mach numbers it is possible to predict the Magnus force on a body of revolution by using the presented cylinder data.

AD Accession No.
Ballistic Research Laboratories, APG
THE MAGNUS FORCE ON A ROTATING CYLINDER IN TRANSONIC CROSS FLOWS
A. S. Platou

BRL Report No. 1150, September 1961

DA Proj No. 503-03-009, OMSC No. 5210.11.140
UNCLASSIFIED Report

UNCLASSIFIED

Projectiles - Exterior Ballistics-Measurements
Projectiles - Aerodynamic Characteristics

This report presents Magnus and drag data on a rotating cylinder mounted perpendicular to various transonic and supersonic flow fields. Data with both laminar and turbulent boundary layers are presented.

The Magnus force data from the cylinder are compared with Magnus force data from various bodies of revolution at high angles of attack. There is good agreement as long as the body of revolution cross Mach number is transonic. The Magnus force is very much dependent on the cross Mach number at the transonic cross flows. At transonic cross Mach numbers it is possible to predict the Magnus force on a body of revolution by using the presented cylinder data.

UNCLASSIFIED